

**Cryo-TEM and Electron Tomography Reveal Leaching-induced Pore Formation in  
ZSM-5 Zeolite**

*Teng Li<sup>‡</sup>, Hanglong Wu<sup>‡</sup>, Johannes Ihli, Zhiqiang Ma, Frank Krumeich, Paul H. H. Bomans,  
Nico A. J. M. Sommerdijk, Heiner Friedrich, Joseph P. Patterson\* and Jeroen A. van  
Bokhoven\**

**Supporting information**

## 1. Characterization methods

### 1.1. Elemental analysis

The Si/Al ratio was measured with a Varian SpectraAA 220FS atomic absorption spectrometer (AAS). Prior to measuring, samples were digested in a 2:3 solution of HF (40%) and HNO<sub>3</sub> (2.5 M) and diluted with distilled water to the required volume.

### 1.2. Powder X-ray diffraction (PXRD)

Powder X-ray diffraction patterns (XRD) were collected on a PANalytical X'Pert PRO MPD diffractometer with Cu K $\alpha$  radiation at room temperature.

### 1.3. <sup>27</sup>Al MAS NMR

Solid-state <sup>27</sup>Al magic angle spinning nuclear magnetic resonance (MAS NMR) measurements were performed on a Bruker 400 UltraShield spectrometer at a resonance frequency of 104.29 MHz. The rotor was spun at 10 kHz and the spectra were recorded with a 4 mm MAS probe, with 3,000 scans averaged for the spectrum. Chemical shifts were referenced to (NH<sub>4</sub>)Al(SO<sub>4</sub>)<sub>2</sub>·12H<sub>2</sub>O for aluminum.

### 1.4. Electron microscopy

TEM images were obtained with Tecnai F30 microscope operated at 300 kV. STEM and EDX measurements were carried out with a Hitachi HD-2700CS microscope operated at 200 kV, which has a secondary electron detector. Please note the Figure 3a is a secondary electron image captured in STEM mode.

### 1.5. Cryogenic transmission electron microscopy (cryo-TEM)

Cryo-TEM Cu grids, R2/2 Quantifoil Jena grids (Quantifoil Micro Tools GmbH) were surface-plasma treated for 40 s using a Cressington 208 carbon coater before use. Samples were taken from the reaction mixture at different time points between 0 and 1440 min. Then, vitrification was carried out using an automated robot (FEI Vitrobot Mark III). The entire sample preparation was performed under nitrogen atmosphere and at 100% humidity to prevent oxidation and drying-induced crystallization, respectively. Vitrified samples were studied on the TU/e CryoTitan, equipped with a field-emission gun operating at 300 kV and a post-column Gatan energy filter. Images were recorded using a post-GIF (Gatan imaging filter) 2×2 k Gatan CCD (charge-coupled device) camera.

### 1.6. Electron tomography

The sample preparation for electron tomography needs the separation of the solid by centrifugation during which a longer time of leaching was expected. As shown in Figure S20, we already obtained a large number of zeolites with big pores in the core at 50 °C even for 25 minutes, which we observed in the later stages in the Cryo-TEM. Therefore, we optimized the leaching conditions and decide to run the experiment at 40 °C for 30 minutes to slow down the dissolution process in case of missing the status of the primary mesopores.

Tomographic tilt series acquisition was conducted with Inspect 3D software (FEI Company) at room temperature. After the tomography, no obvious radiation damage were observed except the focus slightly changed (Figure S16). Alignment and reconstruction was Alignment and reconstruction was carried out in IMOD.] using SIRT with 30 iterations.<sup>1</sup> To remove the artifacts of reconstruction, contrast inversion was performed based on the Equation 1 below:

$$I_{inv} = I_o - (\overline{I_{bg}} + std) \quad (1)$$

Where  $I_{inv}$ ,  $I_0$ ,  $\overline{I_{bg}}$  and  $std$  are the inversed intensity, the original intensity, the averaged background intensity and its standard deviation (Figure S15).

#### Electron tomography acquisition conditions:

Typical angular sampling:  $-66^\circ$  to  $+66^\circ$  at  $2^\circ$  increments;

Magnification: 24000 x;

Defocus:  $-1 \mu\text{m}$ ;

Total image number: 67;

Total electron dose:  $1 e^- / \text{\AA}^2 / \text{image}$ ;

#### 1.7. Segmentation and visualization

Segmentation and visualization of the 3d volume were carried out in Avizo®.<sup>2</sup> A mask was generated by using the brush to manually select the void and solid material areas, respectively, over all the slides. Then this mask was applied to the tomogram to select the target particles and the voids, and the background surrounding these particles was made transparent. The SI visualization movie (Movie S4) shows a volume rendering of two neighboring leached zeolites, where the void distribution can be clearly seen in both particles.

#### 1.8. Focus Ion Beam (FIB)

The zeolite sample was supported on a silicon wafer, then coated with  $\sim 10 \text{ nm}$  Pt using a sputter coating device prior to electron microscope investigation. Before milling, the sample was coated again with a  $\sim 1 \mu\text{m}$  carbon layer to protect the sample. Ion milling was done using a sequence of decreasing milling current to avoid amorphization of the sample. The FIB-SEM investigation of the sample was done in NVision 40 Station. SEM column was operated at 5kV and FIB column was at 30 kV.

#### 1.9. Dissolution kinetics

Zeolite base leaching was carried out using a 0.15 M NaOH solution (35 mL/g zeolite) at  $80^\circ\text{C}$  under constant stirring (500 rpm). Leaching was interrupted at selected time points, by transference of the reaction vessel into an ice/water bath, and the resulting solid product was separated by centrifugation for 5 min at 15,000 rpm. The solid sample was washed three times, dried overnight at  $100^\circ\text{C}$  and then the weight of leached sample was measured. The pH value of the solution was measured by pH meter.

#### 1.10. Particle size distribution

Particle size distribution analysis was performed using an in-house developed Matlab GUI (graphical user interfaces), through which we can obtain the length/width of the particle by manually clicking the two points on the target particle in the image. 100 particles were randomly selected and measured at each time point except time 0, due to the limited amount of particles in the TEM images (See Figure S6 and S16).

## 2. Supplementary figures

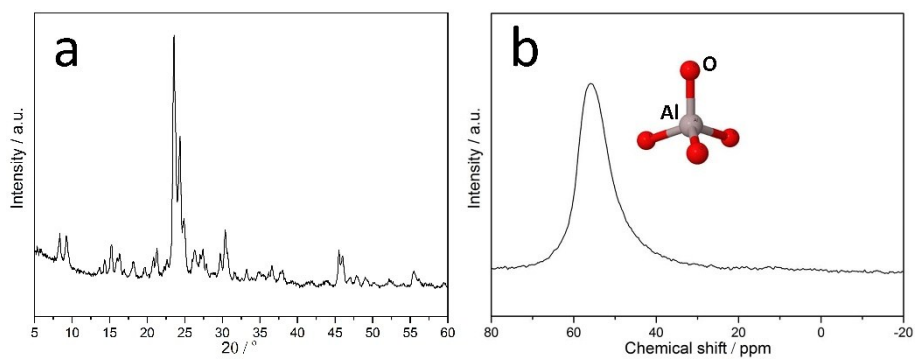


**Figure S1.** (a) XRD pattern and (b)  $^{27}\text{Al}$  MAS NMR spectrum of pristine ZSM-5 zeolites.

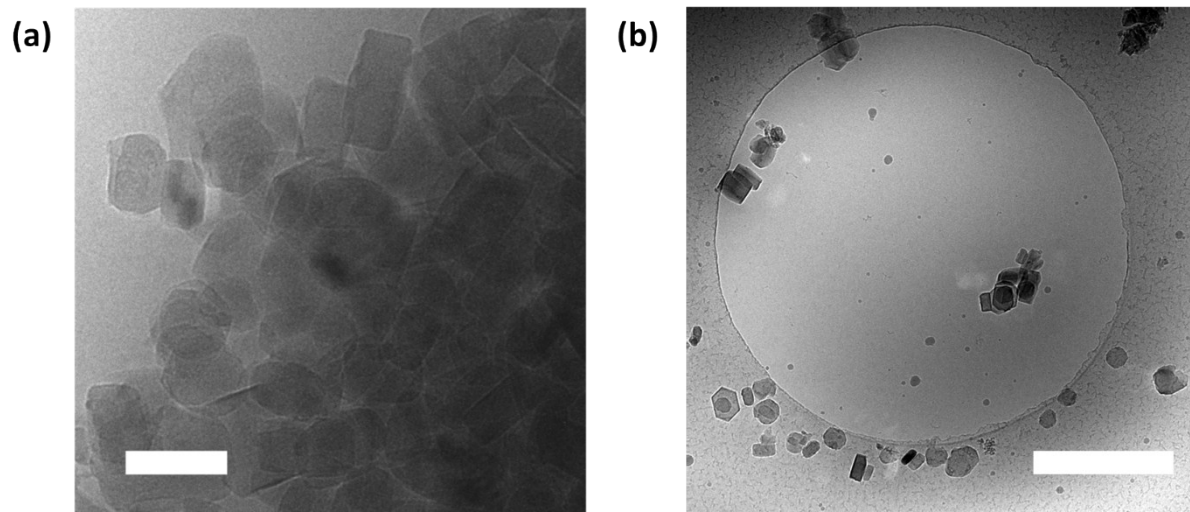


**Figure S2.** Cryo-TEM image of pristine crystals taken at time zero. Scale bars: (a) 100 nm; (b) 800 nm.

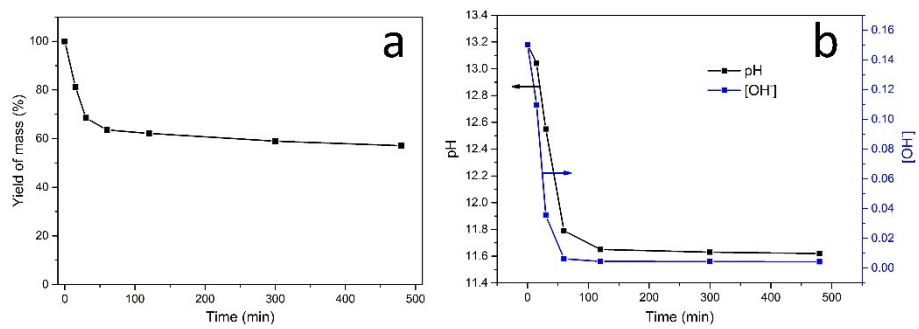


**Figure S3.** (a) Zeolite mass yield as a function of time. (b) pH evolution of the leaching solution.

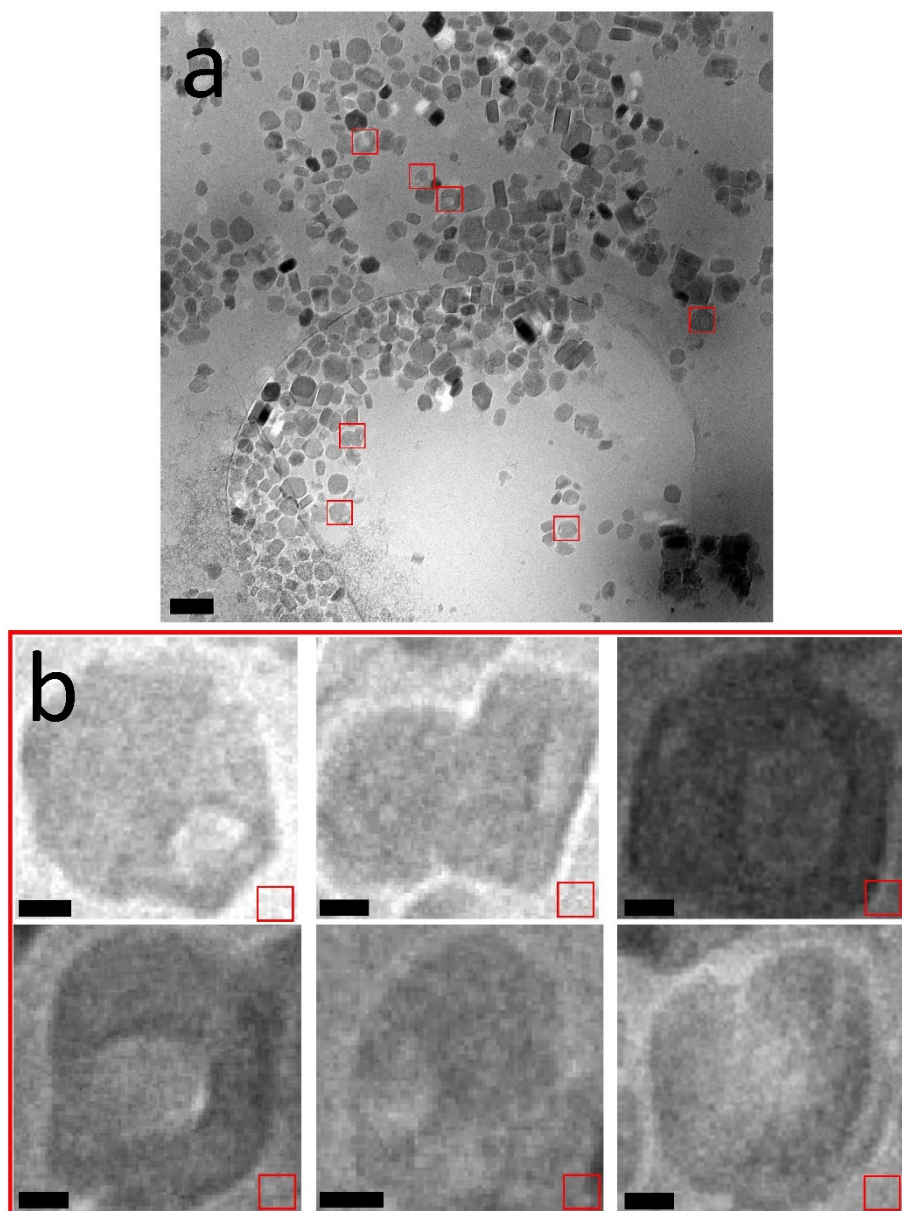


**Figure S4.** Cryo-TEM images of crystals taken after 30 minutes of leaching at 50 °C. (a) Overview and (b) magnification of selected zeolite crystals showing larger pores. Scale bars are 200 nm for (a) and 20 nm for (b).

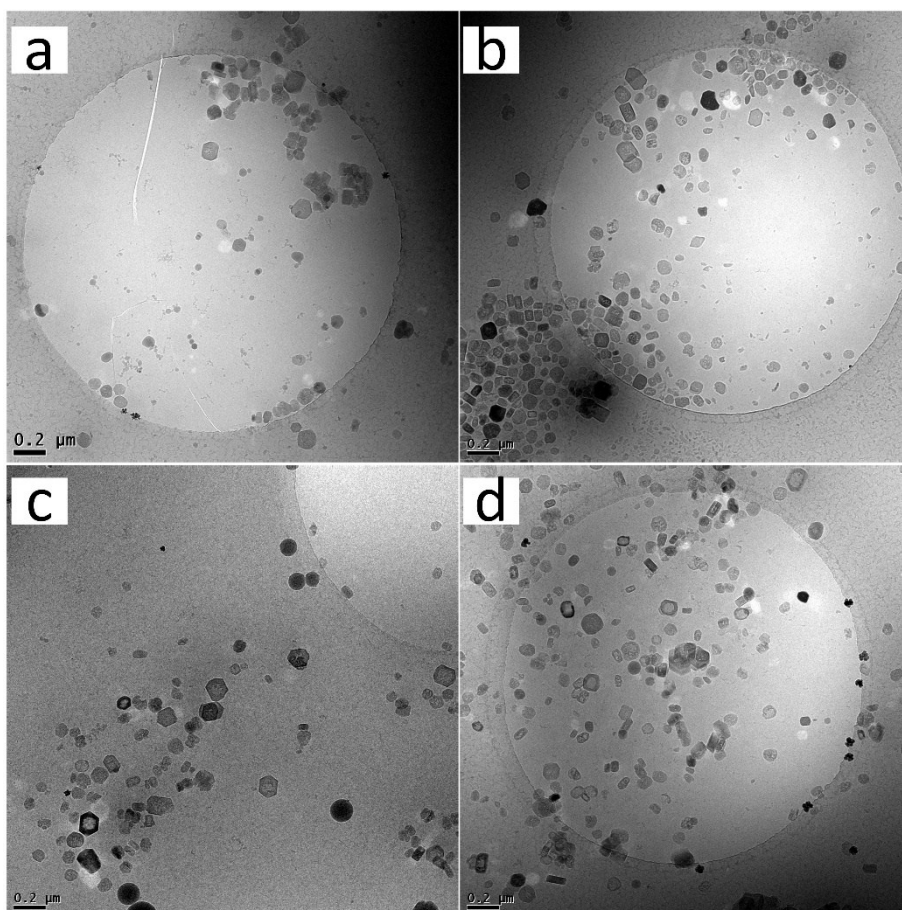


**Figure S5.** Cryo-TEM images of zeolite crystals taken after (a) 120 minutes (b) 275 minutes (c) 470 minutes and (d) 1440 minutes leached at 50 °C. Images presented various extents of pore development during the whole leaching process.

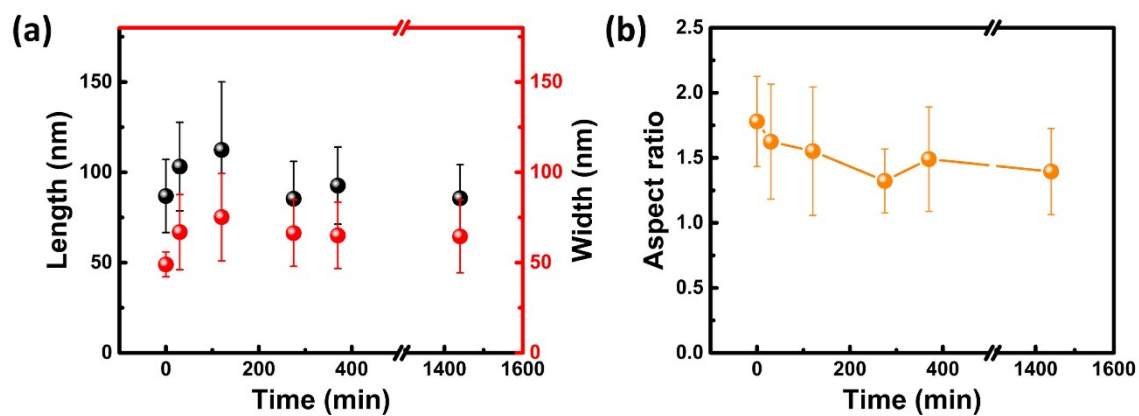


**Figure S6.** The average size of crystals during the leaching at 50 °C. (a) Averaged length, width and (b) aspect ratio distribution over time during the leaching process. See the measured particles with markings in Figures S17.

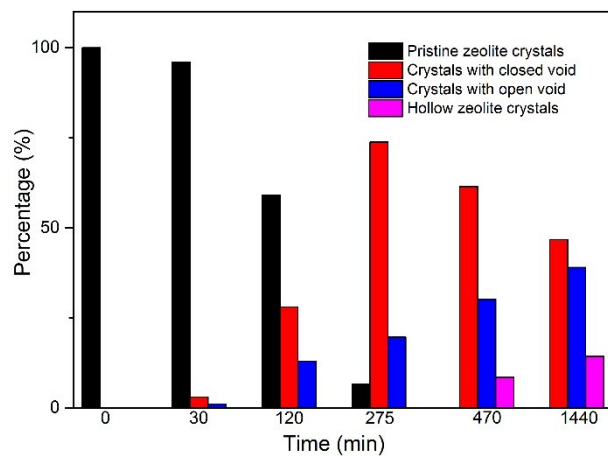


**Figure S7.** Zeolite pore type distribution at selected time point of leaching process (50 °C).

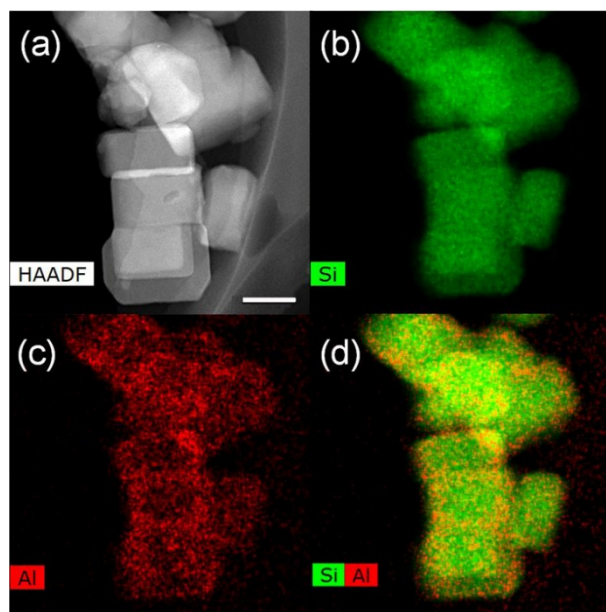


**Figure S8.** HAADF-STEM images of (a) pristine ZSM-5 crystals and EDX maps representing (b) silicon, (c) aluminum, and (d) both. Scale bar 50 nm.<sup>3</sup>

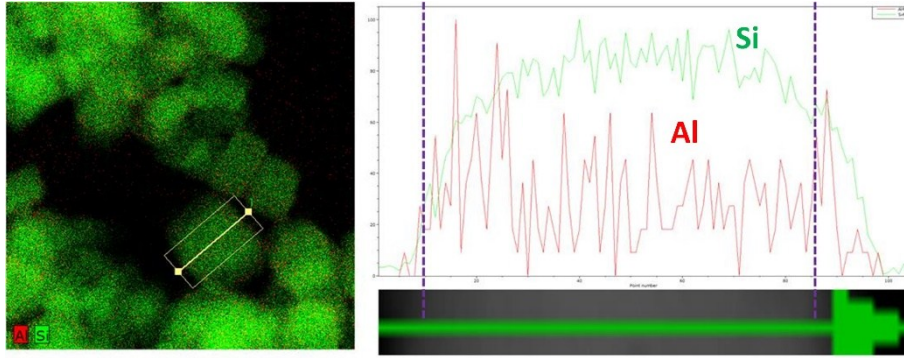


**Figure S9.** EDX line scan to show the difficulty in quantifying aluminium distribution on small crystals.

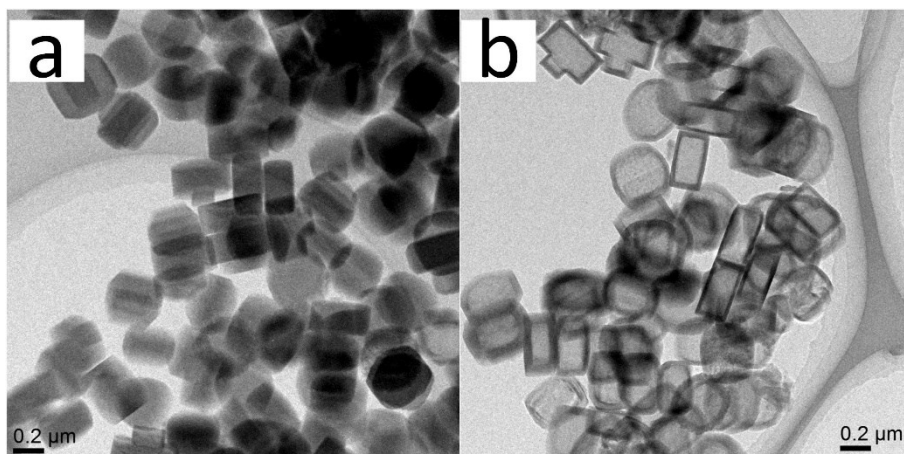


**Figure S10.** TEM images of (a) large ZSM-5 crystals and (b) the corresponding hollow crystals after base leaching.

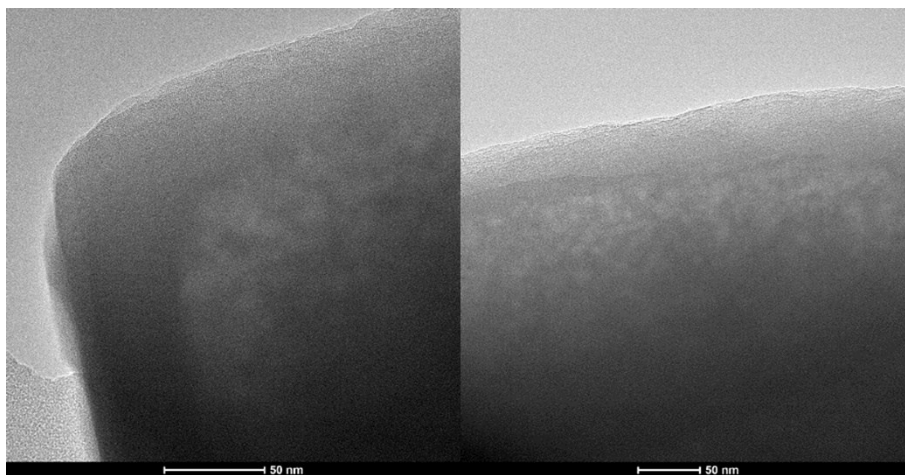


**Figure S11.** TEM images of large ZSM-5 crystals leached for 30 minutes. Similar to small ZSM-5 crystals, larger pores are located close to the rim at an early stage.

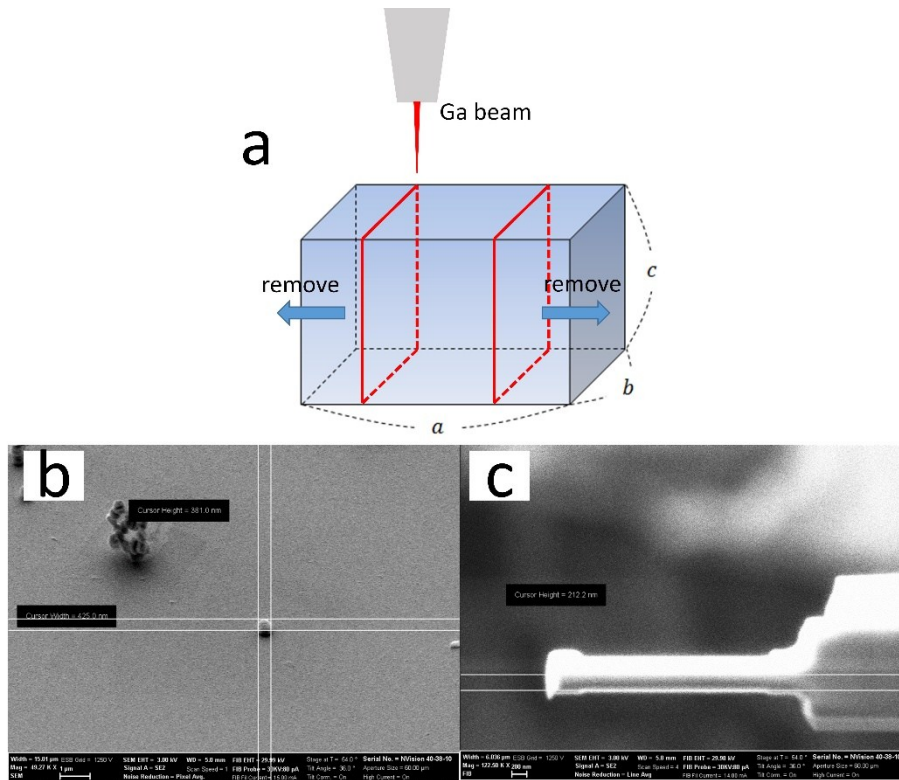
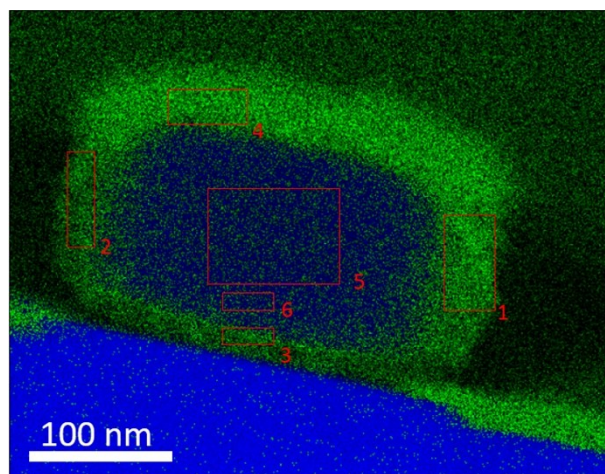
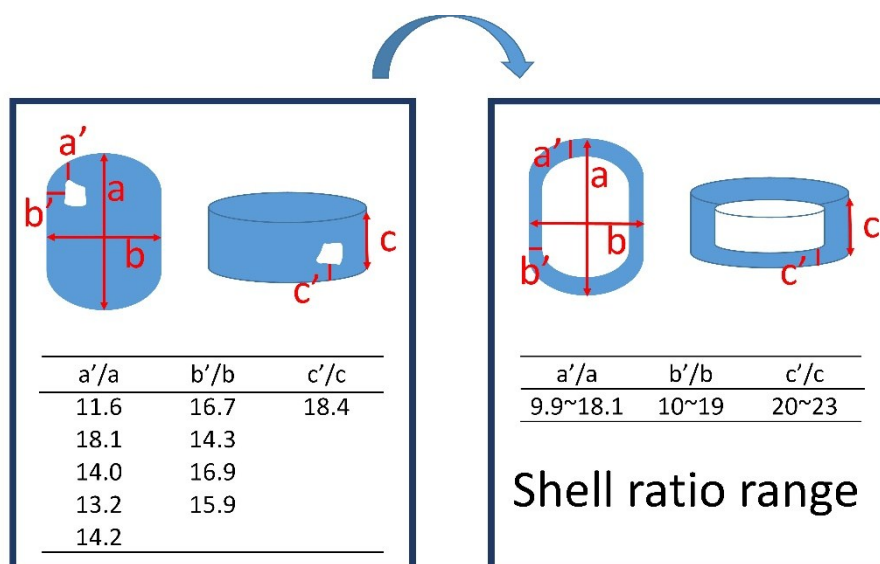


**Figure S12.** (a) A simplified scheme for preparing TEM lamellar of a large ZSM-5 crystal (b) SEM image of the crystal after platinum and carbon deposition (c) SEM image of the crystal after gallium focus ion beam milling.

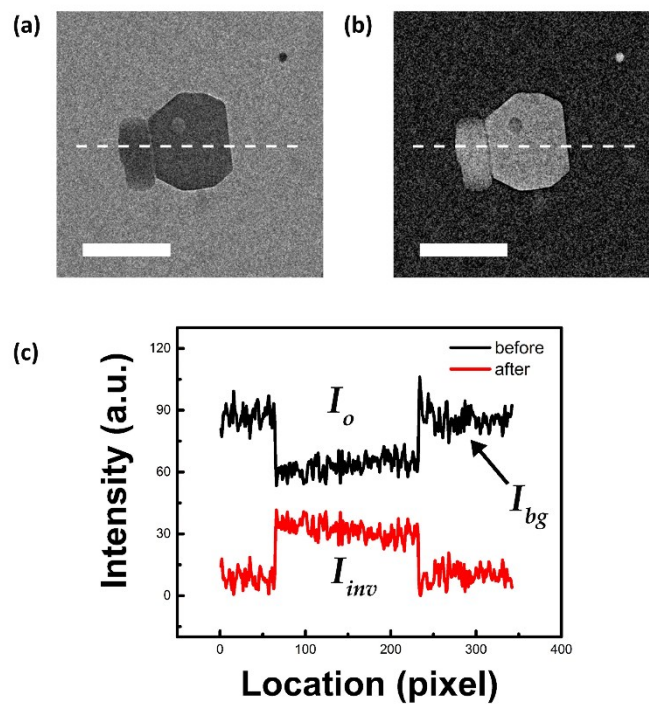


Area	Si (At%)	Al (At%)	Si/Al
1	92.25	7.75	12
2	94.45	5.55	17
3	95.62	4.38	22
4	88.83	11.17	8
5	99.13	0.87	114
6	98.94	1.06	93

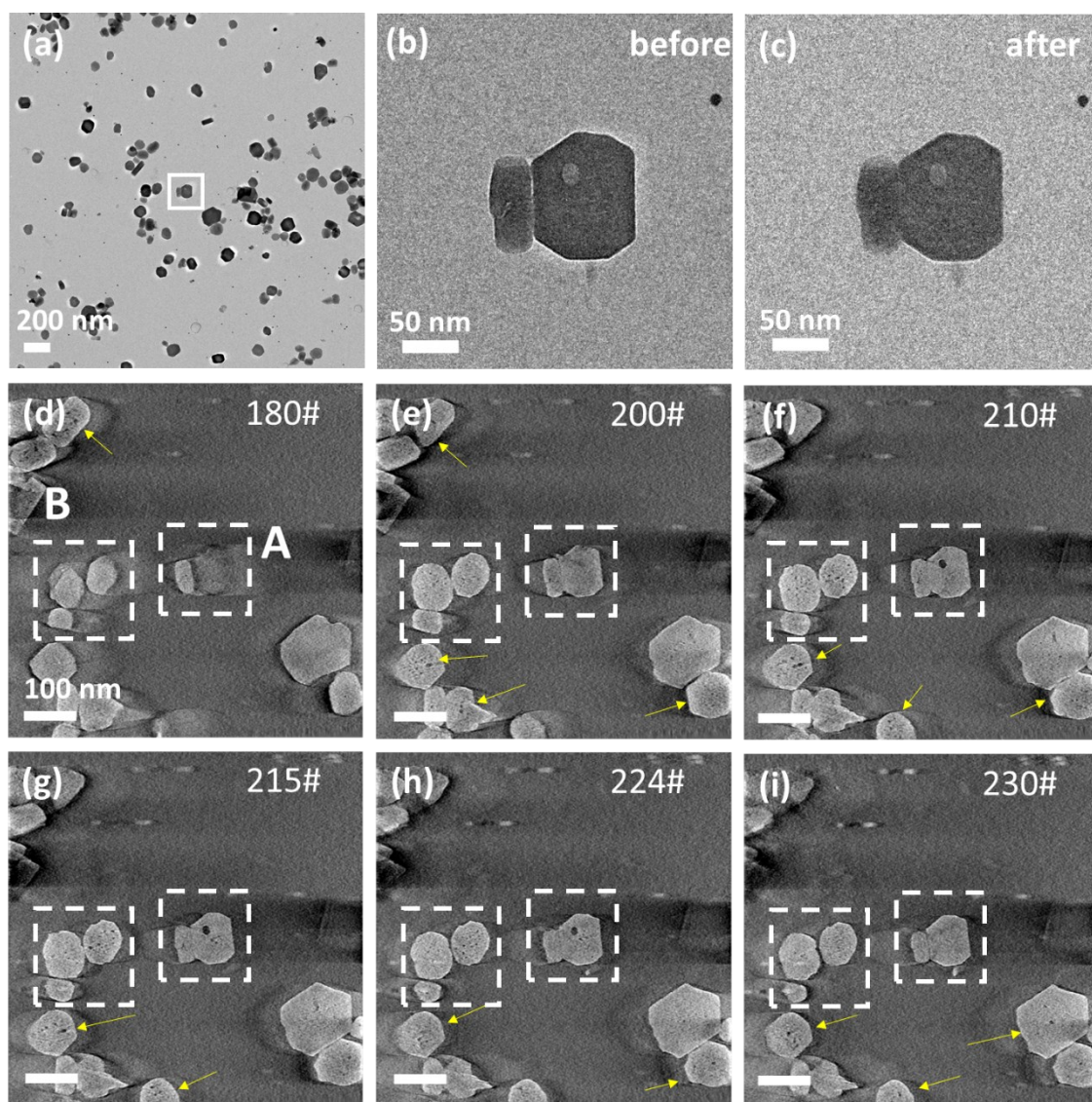
**Figure S13.** EDX point analysis of the cross section.



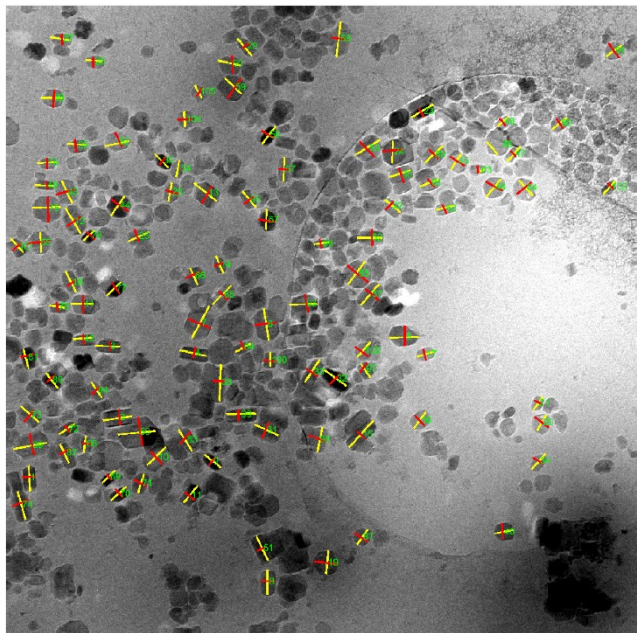
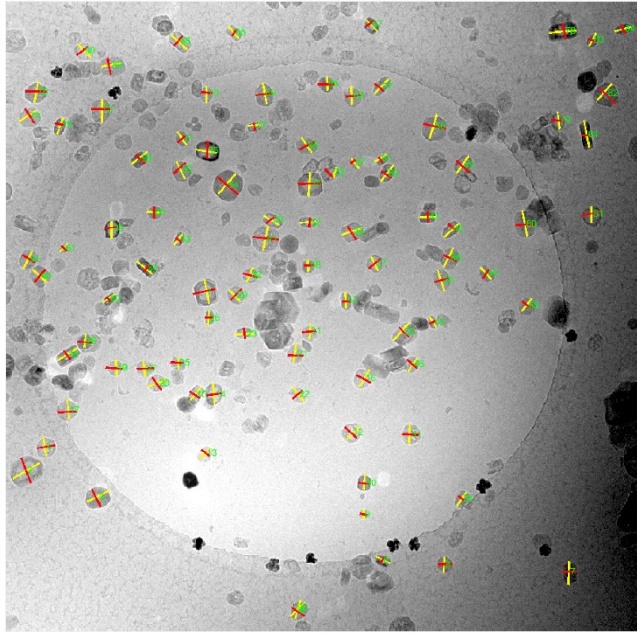
**Figure S14.** A statistics study of the initial larger pore location and the final cavity location within zeolite crystals. It confirms that relatively larger pores formed at early leach stages are located at the surface between aluminum-rich and aluminum-poor parts within individual crystal.



**Figure S15.** Comparison of the same particle before (a) and after (b) contrast inversion. (c) Intensity line profiles calculated from the dashed lines shown in (a) and (b) indicate the contrast is inverted. Scale bar: 100 nm.



**Figure S16.** a) Overview of the area where the electron tomography was performed (Movie S2, S3). (b-c) Comparison of the target particle (highlighted by the white square box A in (a, d-i) before and after the tomography; (d-i) Gallery of z-slices showing different cross sections of a 3DSIRT (simultaneous iterative reconstruction technique) reconstruction (iteration 30) of a tomographic series. The yellow arrows in (d-i) point out the small voids inside other particles besides A and B areas. Scale bar: 100 nm.



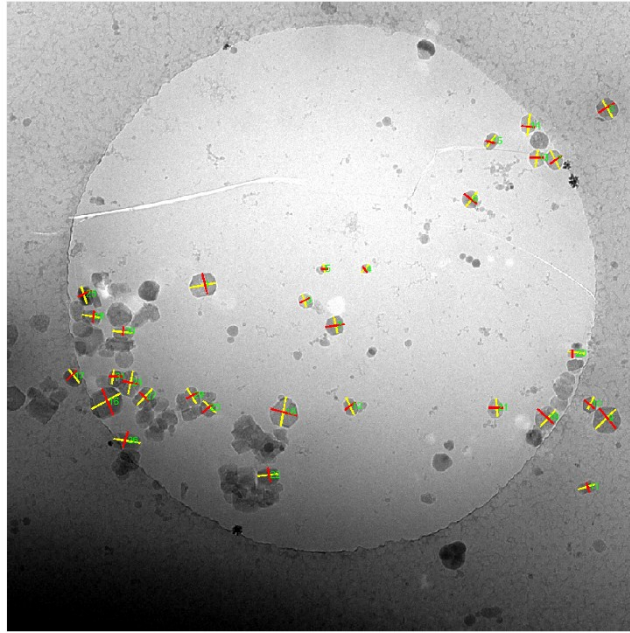


**Figure S17.** Cryo-TEM images (50 °C) with markings for the measurements of lengths and widths for statistical analysis.

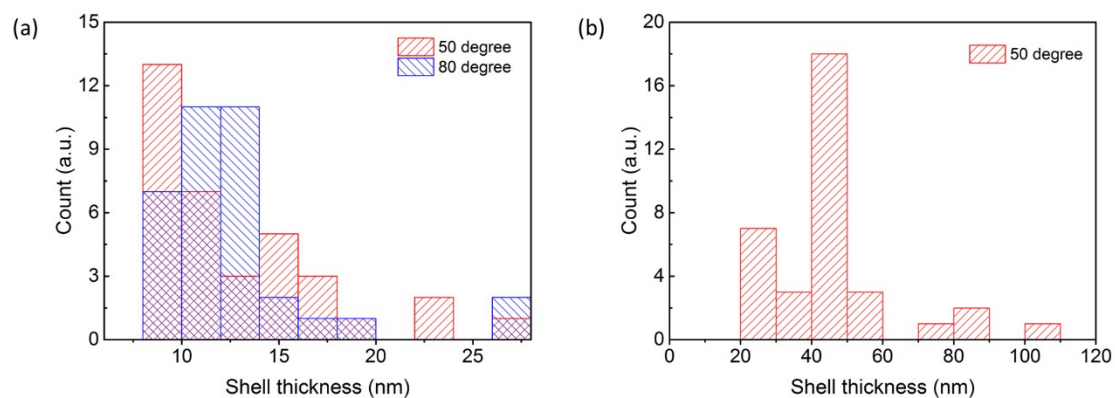


**Figure S18.** Shell thickness distribution in leached zeolites of different particle sizes. (a) Small particles at 50 °C (24 h leaching) and 80 °C (2 h leaching); (b) Big particle at 50 °C. 35 particles for each. The measurement was performed in Digital Micrograph by using the line profile feature.

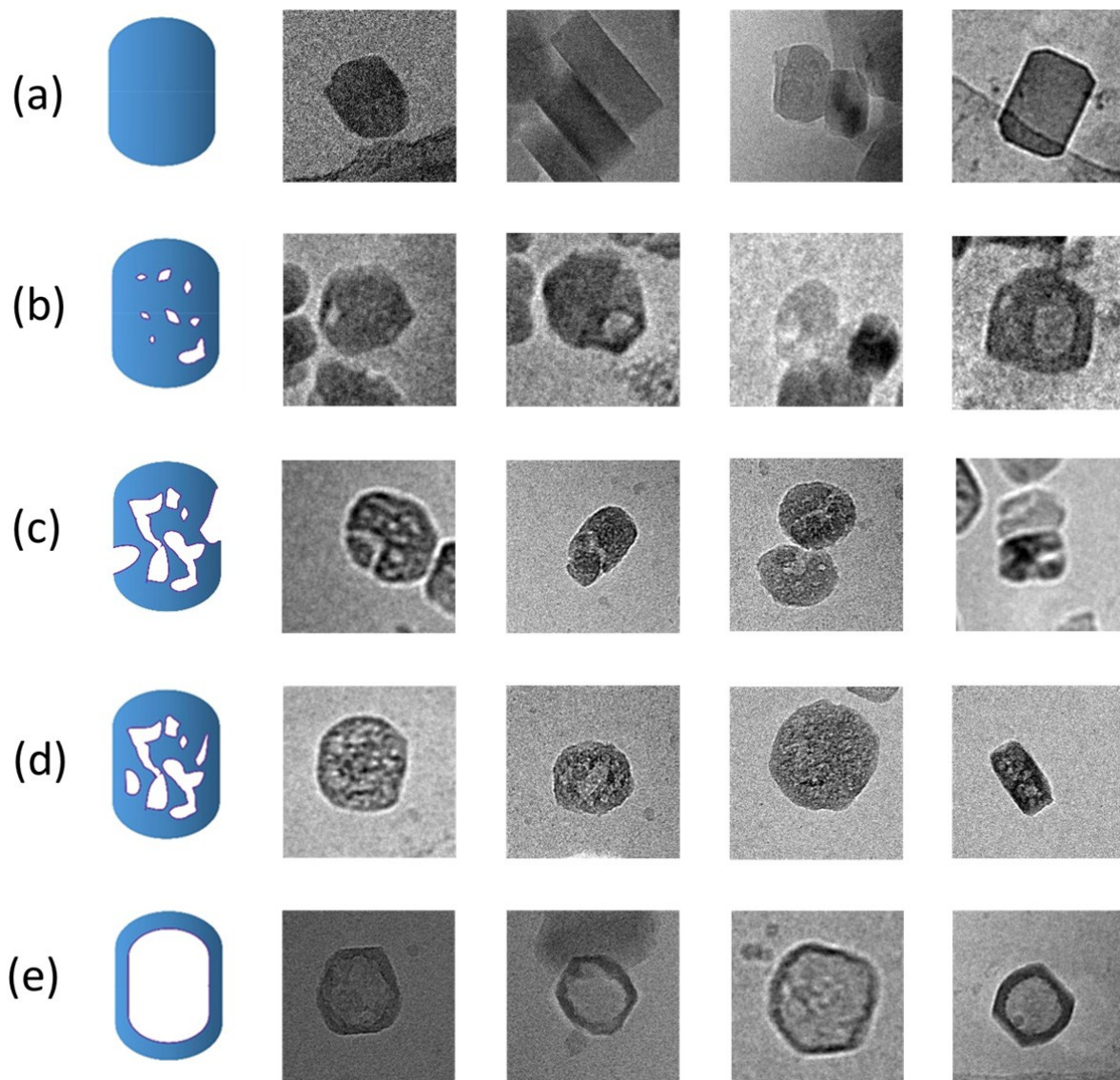


**Figure S19.** Zeolites of different morphologies during leaching. (a) pristine crystals; (b) crystals with the larger pore in the rim and small pore in the core; (c) crystals with pores connected with each other, and the rim part was damaged; (d) crystals with pores connected with each other, and the rim part was nearly intact; (e) hollow zeolite crystals.

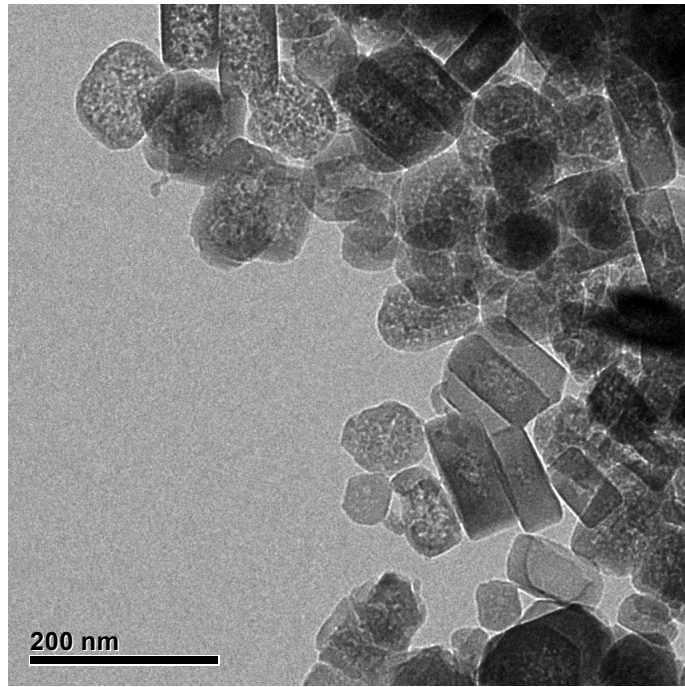


**Figure S20.** Dry-TEM image of zeolites after 25 min leaching at 50 °C

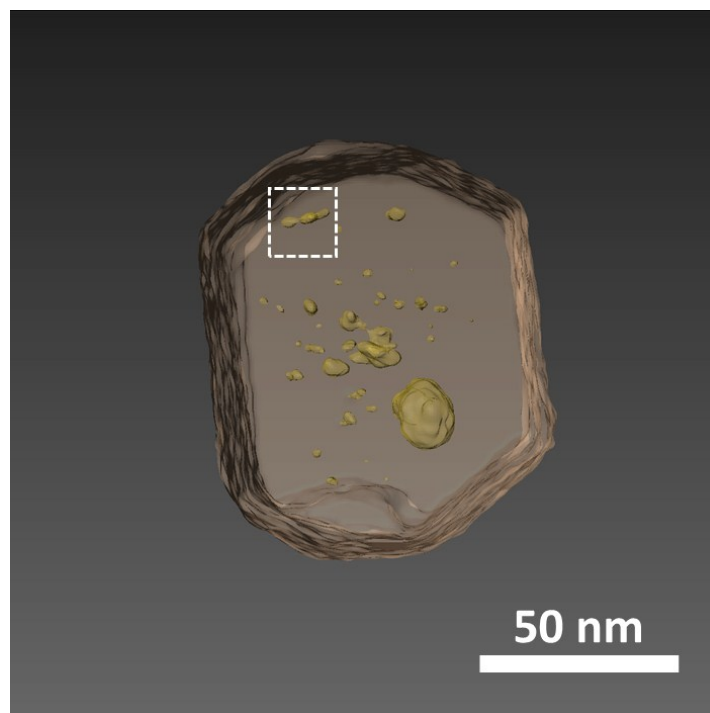


**Figure S21.** Surface rendering of the zeolite in early leaching stages (see Movie S4) shows the coalescence behaviors also exist close to the rim area (highlighted by dashed square box). The mesopores of different sizes can be seen in the core, and evidently many of them are connected with each other. Interestingly, although none of these small pores are connected to the biggest pore close to the rim, we did observe two small pores in the rim area are connected.

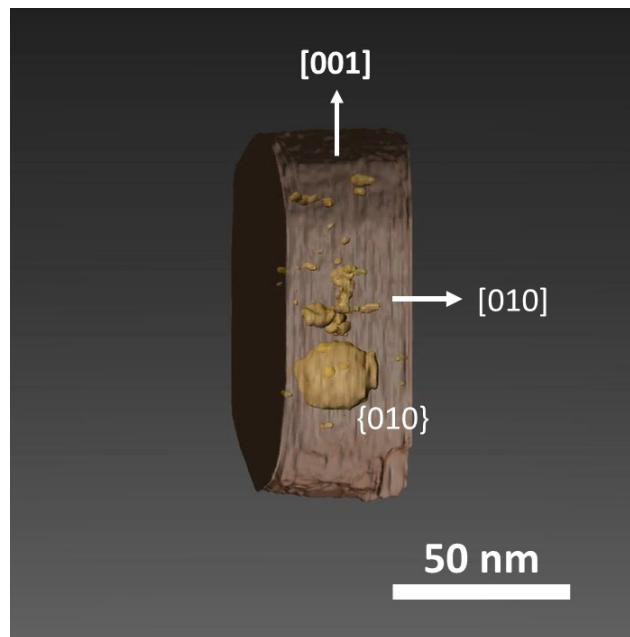


**Figure S22.** Surface rendering of the zeolite in early leaching stages (see Movie S4). We see the flat surface of the big pore is parallel with the  $\{010\}$  surface.

### Supporting Movies:

Movie S1: Tomographic tilt series of leached zeolite crystals.

Movie S2: 3D reconstruction of leached zeolite crystals.

Movie S3: 3D reconstruction of two typical leached zeolite crystals cropped from Movie S2.

Movie S4: Visualization movie of the leached crystals shown in Movie S3.

### References

- 1 J. R. Kremer, D. N. Mastrorade, J. R. McIntosh, *J. Struct. Biol.* 1996, **116**, 71-76.
- 2 B. E. McKenzie, H. Friedrich, M. J. Wirix, J. F. de Visser, O. R. Monaghan, P. H. Bomans, F. Nudelman, S. J. Holder, N. A. Sommerdijk, *Angew. Chem.* 2015, **54**, 2457-2461.
- 3 T. Li, Z. Ma, F. Krumeich, A. J. Knorpp, A. B. Pinar, J. A. Van Bokhoven, *ChemNanoMat*, 2018, **4**, 992-999.